Plasmon-mediated emergence of collective emission and enhanced quantum efficiency in quantum dot films

M. Praveena,[1] Arnab Mukherjee,[1] Murugesan Venkatapathi,[2] and J. K. Basu[1,*]
[1]*Department of Physics, Indian Institute of Science, Bangalore 560012, India*
[2]*Computational Photonics Laboratory, SERC, Indian Institute of Science, Bangalore 560012, India*
(Received 17 May 2015; revised manuscript received 2 August 2015; published 1 December 2015)

We present experimental and theoretical results on monolayer colloidal cadmium selenide quantum dot films embedded with tiny gold nanoparticles. By varying the density of the embedded gold nanoparticles, we were able to engineer a plasmon-mediated crossover from emission quenching to enhancement regime at interparticle distances for which only quenching of emission is expected. This crossover and a nonmonotonic variation of photoluminescence intensity and decay rate, in experiments, is explained in terms of a model for plasmon-mediated collective emission of quantum emitters which points to the emergence of a new regime in plasmon-exciton interactions. The presented methodology to achieve enhancement in optical quantum efficiency for optimal doping of gold nanoparticles in such ultrathin high-density quantum dot films can be beneficial for new-generation displays and photodetectors.

DOI: 10.1103/PhysRevB.92.235403 PACS number(s): 73.20.Mf, 78.20.Bh, 78.55.−m, 78.67.Hc

I. INTRODUCTION

Semiconducting quantum dot (SQD) films or layers are being actively studied as novel materials in various applications ranging from efficient displays and photodetectors to photovoltaics [1–5]. Colloidal quantum dots (CQDs) are specially attractive in this context since they can be prepared over a wide spectral range in highly monodisperse form and can also be easily assembled in to compact mono/multilayered films of arbitrary density using simple methods [6–8]. While the optical [9–11] and electro-optical properties [12–15] of these materials have been well studied, the necessity to push the limits of their quantum efficiencies (QE) for various applications has intensified research in this direction [16–26]. Some theoretical studies [27–30] in the recent past have suggested the possibility of obtaining the strong coupling and collective emission (CE) from an ensemble of quantum emitters like CQDs, mediated by plasmons. Although this methodology offers a powerful scheme to enhance QE in CQD films, there have been no clear demonstrations of the existence of such effects in experiments. In this report, we use a combination of detailed experiments and an appropriate theoretical formalism to demonstrate how surface plasmons of tiny gold nanoparticles (AuNP) can mediate collective emission in compact CQD monolayers. We also demonstrate a nonmonotonic variation of photoluminescence (PL) intensity and decay rate of the CQD films with increasing density of AuNPs (Φ_{Au}) and show, theoretically, how this corresponds to a novel crossover phenomenon arising from competition between plasmon-mediated collective emission, dominating at low Φ_{Au} and predominantly AuNP-CQD near-field energy transfer (ET)–mediated emission at higher Φ_{Au}. The results are significant for several reasons. First, enhanced QE efficiency can be obtained in compact CQD films without disturbing the arrangement of quantum dots (QDs), which makes such a methodology useful for various applications as it is. Furthermore, we have identified an optimum range of ϕ_{Au} where enhanced QE can be achieved. Second, from a fundamental physics point of view, the fact that collective emission emerges with plasmons at a plasmon-exciton separation where quenching is expected points to the emergence of a new regime in plasmon-exciton interactions. Finally, the fact that such collective emission arises with the incorporation of both multiple emitters and multiple NPs is quite significant.

II. EXPERIMENTAL METHODS

The experimental results presented here are based on CQD films consisting of octadecanethiol (ODT) capped cadmium selenide (CdSe) QDs of diameter ($2b$) 3 nm (S series) and 5.2 nm (L series) prepared by the widely used Langmuir-Blodgett (LB) method described earlier [23–25]. Dodecanethiol (DDT) capped AuNPs of diameter ($2a$) 3.5 nm were used as the plasmonic material in the CQD films at various values of Φ_{Au}. Further details of sample preparation are available in [31] and elsewhere [23–25]. For each type of CQDs, compact monolayers at two different densities were prepared on glass slides as shown in Table I. PL measurements were performed in confocal mode using a WiTec Alpha SNOM setup with 488-nm argon (Ar) laser excitation as described earlier [23–25]. Time-resolved PL (TRPL) measurements were performed using a time-correlated single-photon counting system from Horiba Scientific (Fluoro cube-01-NL). All measurements were carried over under room temperature. Figure 1 shows the morphology of the transferred CQD films using a transmission electron microscope (TEM, Technai T20). The TEM images show the presence of a fairly homogeneous CQD layer with randomly dispersed AuNPs.

III. RESULTS AND DISCUSSION

To quantify the TEM images further, we extracted the radial distribution function (RDF) to characterize the extent of ordering and to determine the average interparticle separation between QDs, δ_{QD}, and between QDs and AuNPs, $\delta_{QD-\mathrm{Au}NP}$. A few typical RDFs, which provide estimates of $\delta_{QD-\mathrm{Au}NP}$ and δ_{QD}, are shown in Fig. 2. It is clear, especially from

*basu@physics.iisc.ernet.in

TABLE I. Details of samples.

Sample index[a]	$(N_{CdSe} : N_{Au})$[a]	(h) [b] (nm)	(ρ)[c] (nm^{-2})
Type SH	1:0	(2.555)	3.1×10^{-2}
S_1H	12:1	(2.485)	3.2×10^{-2}
S_2H	6:1	(2.135)	3.1×10^{-2}
S_3H	3:1	(1.715)	3.2×10^{-2}
S_4H	1:1	(...)	.. $\times 10^{-2}$
Type SL	1:0	(4.725)	1.9×10^{-2}
S_1L	12:1	(...)	.. $\times 10^{-2}$
S_2L	6:1	(4.095)	2.0×10^{-2}
S_3L	3:1	(...)	.. $\times 10^{-2}$
S_4L	1:1	(...)	.. $\times 10^{-2}$
Type LH	1:0	(1.715)	3.1×10^{-2}
L_1H	12:1	(1.645)	3.2×10^{-2}
L_2H	6:1	(1.470)	3.2×10^{-2}
L_3H	3:1	(1.400)	3.3×10^{-2}
L_4H	1:1	(...)	.. $\times 10^{-2}$
Type LL	1:0	(3.220)	2.0×10^{-2}
L_1L	12:1	(...)	.. $\times 10^{-2}$
L_2L	6:1	(2.625)	2.0×10^{-2}
L_3L	3:1	(...)	.. $\times 10^{-2}$
L_4L	1:1	(...)	.. $\times 10^{-2}$

[a] S_i, L_i corresponds to S series and L series. H and L correspond to high and low densities, respectively. N_{CdSe} and N_{Au} correspond to the number of CdSe and AuNPs, respectively, as determined from TEM images and stoichiometry.

[b] h is the average surface-surface distance between AuNPs and QDs.

[c] Surface density of QDs in the hybrid films measured from TEM images and also estimated from LB isotherms. The notation (...) implies TEM data is not available for these samples.

Figs. 2(d)–2(e), that incorporation of AuNPs does not change the average δ_{QD} significantly, validating the statement that the light AuNP doping in CQD films did not change the average QD density. Further, using the known values of the capping ligand length of octadecanethiol and dodecanethiol (ODT and DDT), we can estimate the average surface-to-surface separation h between QDs and that between QDs and AuNPs to be 4.7 and 1.4 nm, respectively (also see Table I). The values of δ can also be independently estimated using the respective TEM images. The clear changes in the QD packing

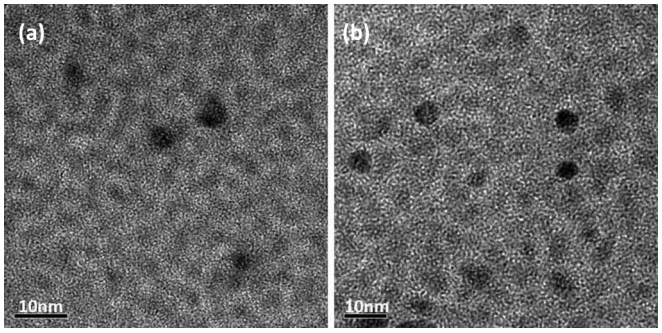

FIG. 1. TEM images of (a) S_2H and (b) L_2H samples. The dark objects are AuNPs and the gray ones correspond to CdSe quantum dots.

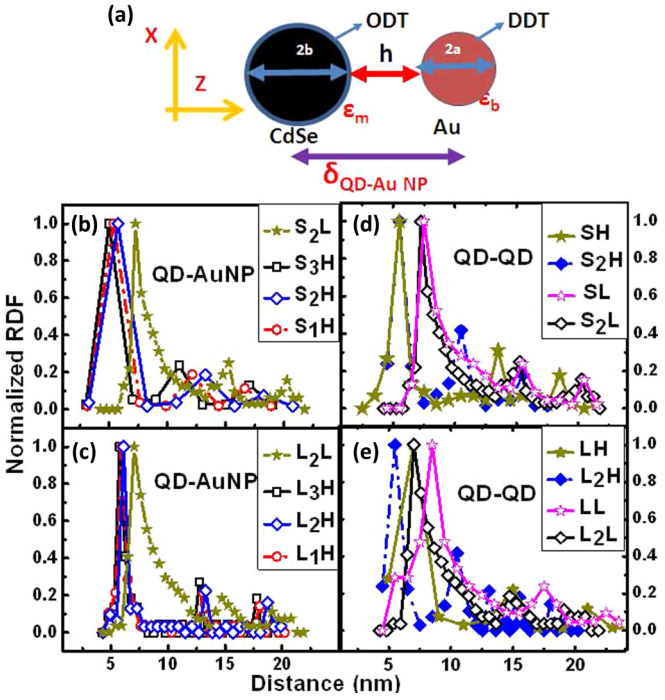

FIG. 2. (Color online) (a) Schematic of the configurations of Au NPs and CdSe QDs in the CQD films. Here $\delta = h + a$. Calculated normalized RDFs representing $\delta_{QD-AuNP}$ of (b) S, (c) L series, and δ_{QD} of (d) S series and (e) L series.

in going from the SL and LL series samples as compared to the SH and LH series samples can be clearly seen from the shift in the first maxima of the respective RDFs. Next we turn our attention to the PL emission from these CQD films. Figure 3 shows a series of PL spectra typical of the various samples indicated in Table I. While the PL spectra for S_4 or L_4 samples show quenching or no enhancement of intensity compared to the pristine CQD monolayer data at similar areal densities, large enhancements are clearly seen for the S_1, S_2 or L_1, L_2 samples containing lower Φ_{Au}. At separation $h \sim 2$ nm, it is expected that the AuNPs would quench the PL from QDs, as seen by several others earlier [22,23,32–34] for isolated QD-AuNP as well as for the high Φ_{Au} case, here. In fact, there seems to be a nonmonotonic trend in PL intensity with increasing Φ_{Au}. This can be seen more clearly in Fig. 4, where the experimental result for the PL enhancement factor $F_{Int}=(I_{hyb}/I_{QD})$ is also summarized, where I_{hyb} is the PL intensity of CQD films doped with AuNP and I_{QD} is the PL intensity of bare CQD film. Very similar trends are observed from independent estimates of PL enhancements, $F_{LT}=\Gamma^R_{hyb}/\Gamma^R_{QD}$, obtained using TRPL measurements, as shown in Fig. 4(b). Here, Γ^R_{hyb} and Γ^R_{QD} are the radiative decay rates of the hybrid and bare QD films, respectively. Further details about the methodology of estimation of F_{LT} has been provided in [31]. The slightly reduced values of F_{LT}, estimated from changes in PL decay rates, in each case, as compared to those obtained from PL intensity measurements is interesting and could be related to the difference in excitation intensity, used for the respective measurements [31]. Several other trends in PL intensity variation can be readily noted

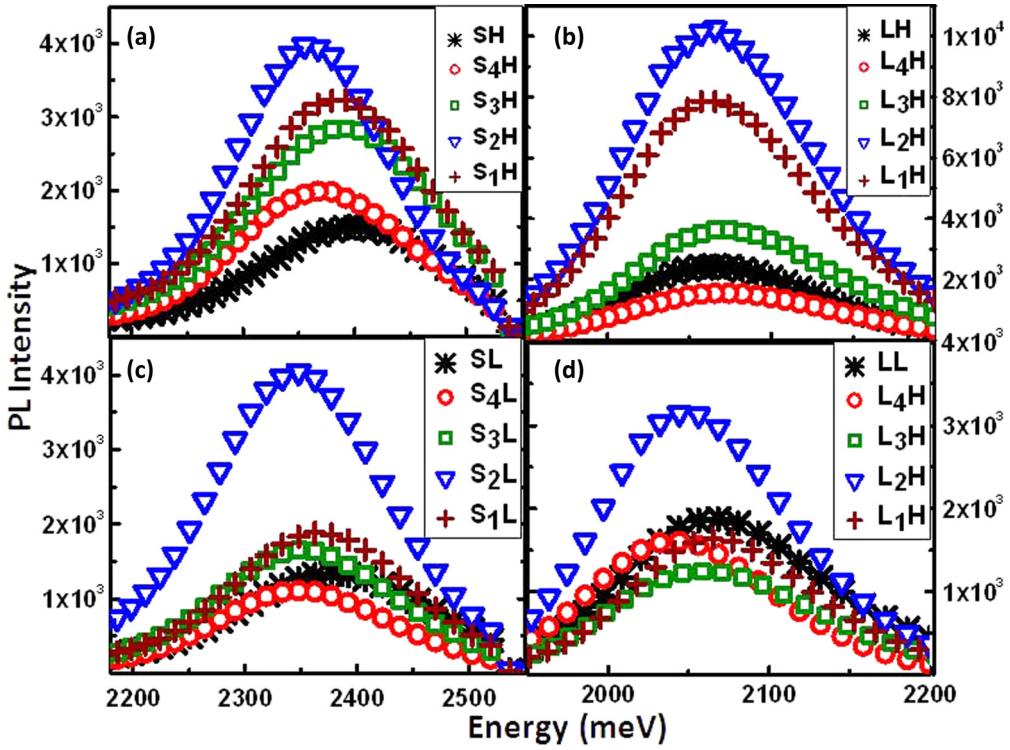

FIG. 3. (Color online) Confocal PL spectra of (a) SH, (b) LH, (c) SL, and (d) LL series CQD films.

in Fig. 4. Reduction in the CQD density in the monolayers (LL and SL series) leads to reduction in the F_{Int}, especially for the off-resonant samples (LL series). This indicates that the observed enhancement depends on AuNP-QD surface-to-surface separation h. In addition, the enhancement effect seems to be independent of the extent of spectral overlap between the AuNP absorbance and PL of the CQDs (see Fig. S2 in the Supplemental Material [31]) and hence the effect is spectrally broadband, at least to the extent that it has been probed here in experiments. Separate measurements (not reported here) seem to suggest that the PL enhancement is weakly dependent on the intrinsic quantum yield (Q) of the CQDs. What is clear from either PL intensity or lifetime measurements is that there seems to be a crossover from a PL enhancement to a quenching regime with increasing doping of the CQD monolayers with AuNPs. The PL enhancement $F_{\mathrm{Int}}(F_{LT})$ seems to be maximized for all cases at $\Phi_{\mathrm{Au}} \sim 0.15$ and decreases with either increasing or decreasing Φ_{Au}. We now set about trying to model the essence of the observed nonintuitive trends of PL intensity and decay rate variation through numerical simulations of the self-energies and collective modes of emission possible. We use a nominal model which contains the essential details of the experimental configuration of a compact CQD monolayer with AuNPs randomly dispersed to obtain a qualitative model to explain the underlying physics of the observed PL enhancement. The diameter of the AuNPs was considered to be 3.5 nm, while that of the QDs was assumed to be 3 nm, similar to the S-series samples in experiments. The interstitial gap h between the AuNP and the QD was assumed to be 1.25 nm. The model was designed to represent the experimental configuration to the extent that it represents the primary exciton-exciton, exciton-plasmon, and plasmon-plasmon interactions likely to be present in the experimental system. Further details about the methodology and the model calculations can be found in [31].

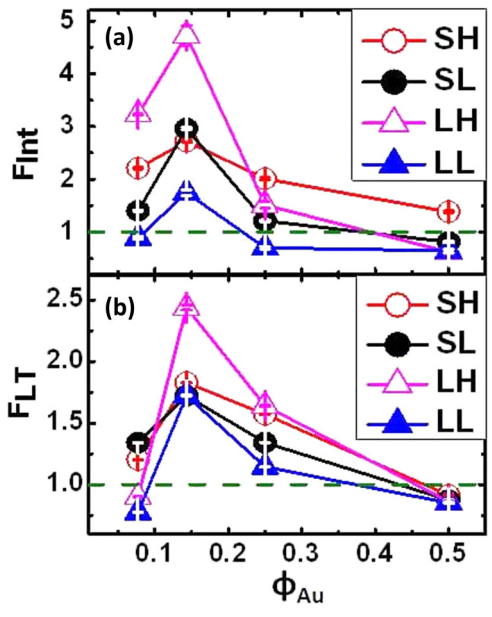

FIG. 4. (Color online) Experimental values of enhancement with respect to Φ_{Au} in respective samples as indicated in the panels: (a) from PL intensity measurements and (b) from TRPL measurement data.

As mentioned before, the extent of PL enhancement seems to depend on the excitation power. This suggests that a sufficient number of QDs have to be excited simultaneously for

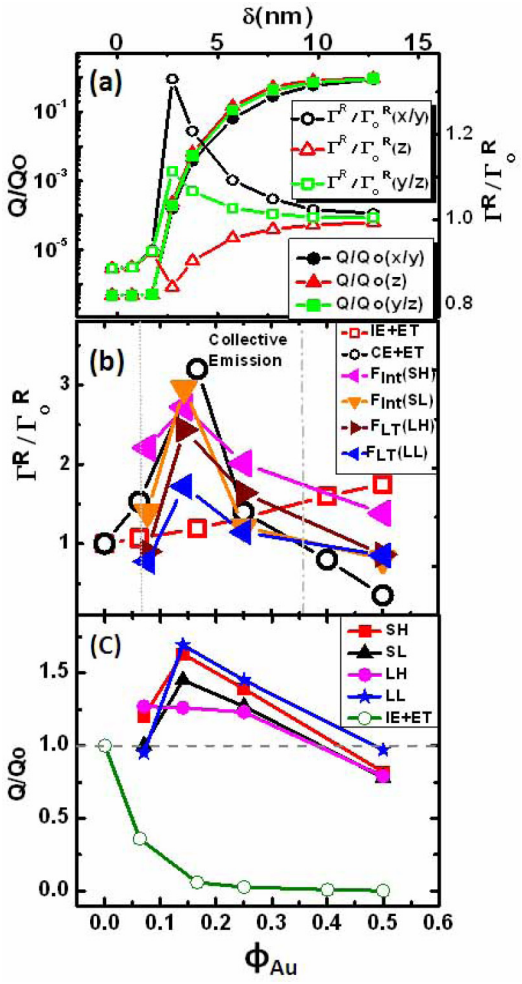

FIG. 5. (Color online) (a) Enhancement in the decay rates for different polarizations of a single photon emitter (SQD parameter) near a AuNP in the case of independent emission. Γ_0^R is the radiative decay rate of the QD without the presence of AuNP. Emission enhancement factor with ϕ_{Au}. Here the gap is 1.25 nm, the quantum yield of bare QD, i.e., Q_o, where CE is collective emission, IE is independent emission, ET is radiation-less loss by energy transfer included. The vertical dotted lines in panel (b) indicate tentative ϕ_{Au} values within which CE dominates ET. (c) The QE values calculated from F_{LT} and compared with those from the IE+ET model.

these large enhancements to manifest. Figure 5(a) shows the distance-dependent decay rates of a single photon emitter (QD in our case) near a AuNP of diameter 3.5 nm. It is obvious that the large enhancements in PL power (Γ^R) observed in experiments are not explained by independent interactions of a QD with a metal nanoparticle distance, $\delta_{QD-\mathrm{Au}NP}$. As shown later, such enhancements of radiative decay rates can emerge from a consideration of collective excitations of the QDs in the monolayer. The collective eigenstates of the excited QDs emerge due to exchange of virtual photons among them, both directly and through the intermediary virtual excitations (plasmons) of the metal particle. These virtual interactions are represented by a set of quantum harmonic oscillators coupled by green tensors in the medium with the metal nanoparticles. This perturbation of the metal particles (and other QDs) to the self-energy of a QD has both radiative and nonradiative components to be evaluated. The evaluation of the collective modes of emission for a set of dipole emitters around a single spherical particle under the long-wavelength approximation was described earlier [27]. This was extended recently to arbitrary heterogeneous mixtures, even on the order of wavelength dimensions, using computational methods [30]. We note that the accuracy of the evaluated collective characteristics can be significantly degraded by a long-wavelength approximation, even in seemingly reasonable cases. The evaluations are averaged over ensembles represented by many random variations in the location and polarization of the interacting dipole emitters, implicitly representing the density of states for collective emission from a structure whose nominal geometrical parameters is known. Each of the collective eigenstates J of a sampled geometry is represented by energy shifts Δ_J and radiative and nonradiative decay rates Γ_J^R, Γ_J^{NR}, respectively. These eigenstates are given by the eigenvalues and eigenvectors of the self-energy matrix $\sum_{jk} = \Delta_{jk} - i\Gamma_{jk}/2$. The diagonal terms of the self-energy matrix Δ_{ii}, Γ_{ii}^R, and Γ_{ii}^{NR} give us the characteristics of the independent emission in the heterogeneous mixture and can be used to deflate the collective effects. The effect of thermal fluctuations and the evaluation of the probabilities of survival of a particular collective mode are described elsewhere. In Fig. 5(b) we show the predicted enhancements in the decay rates for both the case of independent emission and the case of collective emission possible in the QD monolayers and that there is a crossover between the two regimes with Φ_{Au}, in a remarkably similar manner to the experimental observations. At high Φ_{Au} (>0.5) emission seems to be dominated by ET, and it would be difficult to distinguish between independent emission (IE) and collective emission (CE). Most of the experimental reports usually occur in this regime of large ϕ_{Au}. However, the interesting regime lies at $\Phi_{\mathrm{Au}} < 0.5$. In Fig. 5(c), we also show the QE calculated from TRPL measurements for some of our samples. For most of the samples, the QE enhancement trend is similar to F_{LT} or F_{Int} and is quite different from the quenching expected for the IE+ET model. Thus it is clear that the large PL enhancements observed in our experiments, especially for $\Phi_{\mathrm{Au}} \leqslant 0.5$, are due to dominance of CE in the system and cannot be explained only by IE+ET models. It might be noted here that the crossover from quenching to the enhancement regime in the compact CQD monolayers takes place just by changing Φ_{Au} without significant change in $\delta_{QD-\mathrm{Au}NP}$ or δ_{QD}. Our work thus represents a clear experimental demonstration of the existence of CE in emitters mediated by plasmons. Furthermore, while several recent theoretical models predict the onset of CE for either relatively larger separation between the emitters and metal nanoparticles [28,30] or for separations similar to our configuration [29] but for very large emitter-to-nanoparticle ratios, our model captures the experimental results with separations in a regime where quenching is expected for IE models and with fairly small emitter-to-nanoparticle ratios. Moreover, none of the reported theoretical models have treated both multiple emitters and multiple metal nanoparticles, with the exception of our recent report [30]. Although the calculations have been performed for a particular size of QD and AuNP, we believe that the effect exists over a broader range of sizes. In fact the collective emission effect seems to exist in a band of sizes for AuNPs, i.e., it diminishes above

and below a certain critical diameter of the particles. Exact quantitative matching with experimental data would involve consideration of the actual detailed experimental parameters, which is outside the scope of this work. In addition, our close calculations also indicate that the emergence of CE depends sensitively on the excited rate and is distinguishable at low excited rates, as evidenced from Fig. 4(b). This aspect will be dealt with, in a separate work.

IV. CONCLUSION

In conclusion, we presented experimental and theoretical results on the photoluminescence of CdSe quantum dot films embedded with tiny gold nanoparticles and demonstrated an emergence of a plasmon-mediated collective-emission-dominated regime of QDs. The CE regime was engineered only through variation of the density of AuNPs in the compact CQD films, without changing the QD density. The CE observed in the CQD films seems to be spectrally broadband, although its magnitude is larger in the case where the QD emission spectral overlap is minimized with respect to the surface plasmon resonance of the embedded AuNPs. Furthermore, we discuss the regimes where this phenomenon is likely to be most effective. Our results suggest methods to achieve enhancement in optical quantum efficiency in such quantum dot films, with potential significance for new-generation displays and photodetectors.

ACKNOWLEDGMENTS

We acknowledge the Department of Science and Technology (Nanomission), India, for financial support and the Advanced Facility for Microscopy and Microanalysis, Indian Institute of Science, Bangalore, for access to TEM and TRF measurements. M.P. acknowledges University Grants Commission, India for financial support. A.M. acknowledges the Department Of Science & Technology, Nanomission, India, for financial support.

[1] C. R. Kagan, C. B. Murray, and M. G. Bawendi, Phys. Rev. B **54**, 8633 (1996).
[2] H. A. Atwater and A. Polman, Nat. Mater. **9**, 205 (2010).
[3] G. J. Supran, K. W. Song, G. W. Hwang, R. E. Correa, J. Scherer, E. A. Dauler, Y. Shirasaki, M. G. Bawendi, and V. Bulović, Adv. Mater. **27**, 1437 (2015).
[4] D. V. Talapin and C. B. Murray, Science **310**, 86 (2005).
[5] N. C. Giebink, G. P. Wiederrecht, M. R. Wasielewski, and S. R. Forrest, Phys. Rev. B **83**, 195326 (2011).
[6] K. M. Gattas-Asfura, C. A. Constantine, M. J. Lynn, D. A. Thimann, X. Ji, and R. M. Leblanc, J. Am. Chem. Soc. **127**, 14640 (2005).
[7] M. Achermann, M. A. Petruska, S. A. Crooker, and V. I. Klimov, J. Phys. Chem. B **107**, 13782 (2003).
[8] V. Klimov, A. Mikhailovsky, S. Xu, A. Malko, J. Hollingsworth, C. Leatherdale, H.-J. Eisler, and M. Bawendi, Science **290**, 314 (2000).
[9] J. M. Luther, P. K. Jain, T. Ewers, and A. P. Alivisatos, Nat. Mater. **10**, 361 (2011).
[10] D. C. Hannah, N. J. Dunn, S. Ithurria, D. V. Talapin, L. X. Chen, M. Pelton, G. C. Schatz, and R. D. Schaller, Phys. Rev. Lett. **107**, 177403 (2011).
[11] A. O. Govorov, G. W. Bryant, W. Zhang, T. Skeini, J. Lee, N. A. Kotov, J. M. Slocik, and R. R. Naik, Nano Lett. **6**, 984 (2006).
[12] G. Konstantatos, M. Badioli, L. Gaudreau, J. Osmond, M. Bernechea, F. P. G. de Arquer, F. Gatti, and F. H. Koppens, Nat. Nanotechnol. **7**, 363 (2012).
[13] S. Chanyawadee, R. T. Harley, M. Henini, D. V. Talapin, and P. G. Lagoudakis, Phys. Rev. Lett. **102**, 077402 (2009).
[14] R. Y. Wang, J. P. Feser, J.-S. Lee, D. V. Talapin, R. Segalman, and A. Majumdar, Nano Lett. **8**, 2283 (2008).
[15] W. Zhou, M. Dridi, J. Y. Suh, C. H. Kim, D. T. Co, M. R. Wasielewski, G. C. Schatz, T. W. Odom *et al.*, Nat. Nanotechnol. **8**, 506 (2013).
[16] S. Jin, H.-J. Son, O. K. Farha, G. P. Wiederrecht, and J. T. Hupp, J. Am. Chem. Soc. **135**, 955 (2013).
[17] M. Liu, T.-W. Lee, S. K. Gray, P. Guyot-Sionnest, and M. Pelton, Phys. Rev. Lett. **102**, 107401 (2009).
[18] A. Akimov, A. Mukherjee, C. Yu, D. Chang, A. Zibrov, P. Hemmer, H. Park, and M. Lukin, Nature (London) **450**, 402 (2007).
[19] M. Tame, K. McEnery, Ş. Özdemir, J. Lee, S. Maier, and M. Kim, Nat. Phys. **9**, 329 (2013).
[20] O. Chen, J. Zhao, V. P. Chauhan, J. Cui, C. Wong, D. K. Harris, H. Wei, H.-S. Han, D. Fukumura, R. K. Jain *et al.*, Nat. Mater. **12**, 445 (2013).
[21] Y. Yang, Y. Zheng, W. Cao, A. Titov, J. Hyvonen, J. R. Manders, J. Xue, P. H. Holloway, and L. Qian, Nat. Photonics **9**, 259 (2015).
[22] K. Hosoki, T. Tayagaki, S. Yamamoto, K. Matsuda, and Y. Kanemitsu, Phys. Rev. Lett. **100**, 207404 (2008).
[23] M. Haridas, L. N. Tripathi, and J. K. Basu, Appl. Phys. Lett. **98**, 063305 (2011).
[24] L. N.Tripathi, M. Praveena, and J. K. Basu, Plasmonics **8**, 657 (2013).
[25] L. N. Tripathi, M. Praveena, P. Valson, and J. K. Basu, Appl. Phys. Lett. **105**, 163106 (2014).
[26] M. Haridas, J. K. Basu, A. Tiwari, and M. Venkatapathi, J. Appl. Phys. **114**, 064305 (2013).
[27] V. N. Pustovit and T. V. Shahbazyan, Phys. Rev. B **82**, 075429 (2010).
[28] V. N. Pustovit and T. V. Shahbazyan, Phys. Rev. Lett. **102**, 077401 (2009).
[29] A. Delga, J. Feist, J. Bravo-Abad, and F. J. Garcia-Vidal, Phys. Rev. Lett. **112**, 253601 (2014).
[30] M. Venkatapathi, JOSA B **31**, 3153 (2014).
[31] See Supplemental Material at http://link.aps.org/supplemental/10.1103/PhysRevB.92.235403 for more details on the preparation of materials, analysis, model calculations, and related additional figures.
[32] Z. Gueroui and A. Libchaber, Phys. Rev. Lett. **93**, 166108 (2004).
[33] E. Dulkeith, A. C. Morteani, T. Niedereichholz, T. A. Klar, J. Feldmann, S. A. Levi, F. C. J. M. vanVeggel, D. N. Reinhoudt, M. Moller, and D. I. Gittins, Phys. Rev. Lett. **89**, 203002 (2002).
[34] P. Anger, P. Bharadwaj, and L. Novotny, Phys. Rev. Lett. **96**, 113002 (2006).